10628 *Macromolecules* **2010**, *43*, 10628–10635
DOI: 10.1021/ma1021055

Macromolecules
ARTICLE

Multistimuli Responsive Organosilica Hybrid Nanoparticles Based on Poly(ether amine)

Rui Wang, Xuesong Jiang,* Chunfeng Di, and Jie Yin*

School of Chemistry & Chemical Technology, State Key Laboratory for Metal Matrix Composite Materials, Shanghai Jiao Tong University, Shanghai 200240, People's Republic of China

Received September 11, 2010; Revised Manuscript Received November 8, 2010

ABSTRACT: We demonstrated here novel multistimuli responsive organosilica hybrid nanopaticles ($SiO_{1.5}$-gPEA NPs) based on graft poly(ether amine)s (gPEAs). Poly(ether amine)s comprised of trimethoxysilyl moieties (TMS-gPEAs) were synthesized via nucleophilic substitution/ring-opening reaction of commercial poly(propylene glycol) diglycidyl ether, Jeffamine L100 and 2-aminoethanolthiol, followed by introducing trimethoxysilyl moieties (TMS) into side-chain via "thiol−ene" reaction. The obtained TMS-gPEAs could be dispersed directly in water to form the core-cross-linked hybrid nanoparticles ($SiO_{1.5}$-gPEA NPs) with diameter of about 20 nm, which was revealed by TEM and DLS. These obtained $SiO_{1.5}$-gPEA NPs in aqueous solution were responsive to temperature, pH and ionic strength with tunable cloud point (CP). Simultaneously, $SiO_{1.5}$-gPEA NPs could encapsulate hydrophobic guest molecule Nile Red in water. It is interesting that $SiO_{1.5}$-gPEA NPs can sequester the hydrophilic dyes selectively: $SiO_{1.5}$-gPEA11 NPs could transfer only Rose Bengal (RB) reversibly from the aqueous mixture of RB and Rhodamine 6G (R6G) to toluene, which was controlled by temperature. These characteristics will give $SiO_{1.5}$-gPEAs potential in smart separation.

Introduction

Organic−inorganic hybrid nanomaterials have attracted much attention for their potential application in optics, mechanics, electronics, energy, environmental areas.[1−7] These hybrids combining both organic and inorganic materials do not only represent a creative alternative to design new materials and compounds, but their improved features allow the development of innovative industrial application. As the important inorganic component, silica or silsesquioxanes is widely used in the variety of hybrid material.[6,8−10] The introduction of inorganic silica network will enhance the rigid nature of the nanomaterials, resulting in excellent stability even in harsh condition.[9,11] By providing reinforcement to the weak intermolecular interactions that facilitate polymer micelle assembly and existence, the cross-linked core offers stability to the nanostructured assemblies. Furthermore, silica was approved as safe by the U.S. Food and Drug Administration (FDA). So silica-based nanomaterials have broadened their applications in adsorption, catalysis, sensors and medicine.[12−19]

On the other hand, a lot of research has been carried out in the promising field of smart materials, i.e., polymeric nanoparticles that possess the property of response to external stimulus such as temperature, pH or ionic strength. These materials are of great interest for their unique and outstanding physical and chemical properties which are suitable for applications in oil recovery, sensors, and drug delivery.[20−27] Polymeric nanoparticles can encapsulate guest molecules of poor solubility, low stability, or undesirable pharmaceutical properties. However, most of the polymer nanoparticles fabricated by self-assembly were not stable enough, which limits their application in some fields such as drug delivery.[10,28,29] So it is necessary to improve their stabilization to avoid disintegration of the aggregation at low concentration or upon environmental changes. The incorporation of inorganic component containing silica or silsesquioxanes into polymeric nanoparticles is an easy and convenient approach. One such approach involves the covalent incorporation of trialkoxysilane functionalities into the particle's building blocks, followed by hydrolyzation and polycondensation to form the core or shell cross-linked polymeric nanoparticles.[5,8,30−33] Several researches have been carried out on the stimuli-responsive hybrid nanoparticles.[16,34−38]

On the basis of the amphiphilic responsive poly(ether amine)s (PEAs) developed by our group,[39−42] we demonstrated novel multistimuli responsive organosilica hybrid nanoparticles in this text. With the excellent amphiphilic property and sharp response to temperature and pH, PEAs could be synthesized via nucleophilic substitution/ring-opening reaction of epoxy and amine groups, which possesses characteristics of "click-chemistry". Here, we introduced trimethoxysilyl (TMS) moieties into the side-chain of the graft poly(ether amine) containing thiol groups (gPEA-SH) via "thiol−ene" reaction.[43] The obtained TMS-gPEAs could be dispersed directly in water to form polymer nanoparticles with hydrophobic PPO and TMS as core and hydrophilic L100 as shell. The subsequent cross-linking of TMS moieties into silsesquioxane networks resulted in formation of the hybrid polymer nanoparticles ($SiO_{1.5}$-gPEA NPs), which exhibit multiresponse to temperature, pH and ionic strength with tunable cloud point (CP). After investigating the formation of these hybrid nanoparticles and their responsive behavior, we tested their properties as container. It is interesting that besides hydrophobic guest molecules, $SiO_{1.5}$-gPEA NPs can encapsulate hydrophilic dyes with unique selectivity.

Experimental Section

Materials. Poly(propylene glycol) diglycidyl ether (PPO−DE, Aldrich, M_n = 640 g/mol), Jeffamine L100 (Huntsman, M_n = 1000 g/mol), 2-aminoethanethiol (AET, TCI Chemical Reagent),

*Corresponding authors. E-mail: (X.J.) ponygle@sjtu.edu.cn; (J.Y.) jyin@sjtu.edu.cn. Telephone: +86-21-54743268. Fax: +86-21-54747445.

 Published on Web 11/24/2010

Table 1. Composition and Molecular Weight Data of gPEA-SHs

	molar ratio					
polymer[a]	AET	Jaffamine L100	PPO−DE	M_n ($\times 10^4$)[b]	M_w/M_n[b]	products of thiol−ene reaction
gPEA-SH11	1	1	2	1.2	2.61	TMS-gPEA11
gPEA-SH12	1	2	3	0.9	1.90	TMS-gPEA12
gPEA-SH13	1	3	4	1.2	2.58	TMS-gPEA13

[a] gPEA-SH*xy*, where *x*, *y* represent the molar ratio of the raw AET and Jaffamine L100, respectively. [b] Molecular weight and molecular weight polydispersity were measured by GPC.

Scheme 1. Synthesis Process for TMS-gPEAs

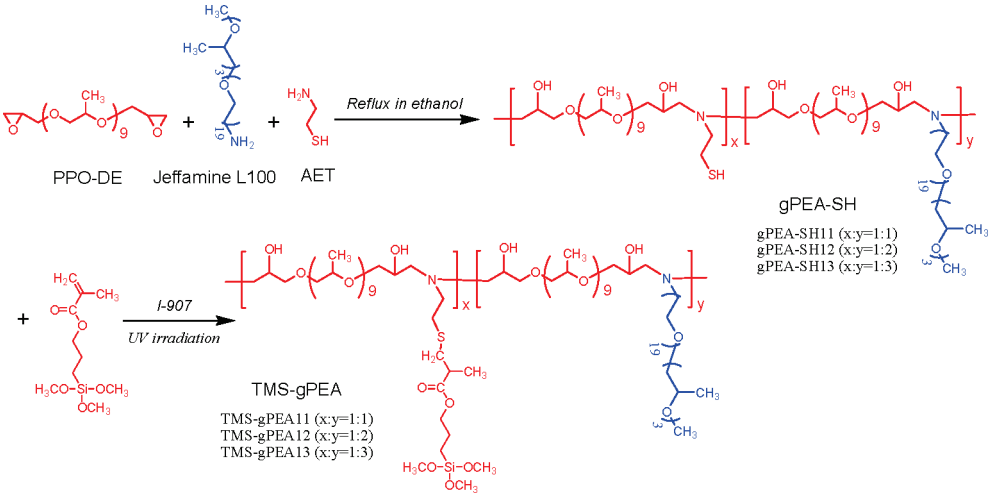

3-(methacryloylpropyl)trimethoxysilane (MPS, Alfa Aesar), Photoinitiator I-907 (Tronly. Changzhou, China), Nile Red (TCI Chemical Reagent), Rhodamine 6G (Aldrich), were used as received. Rose Bengal (RB), Amido Black 10B (10B), Bordeaux R (BoR), Methyl Orange (MO) and Calcein (Cl) were bought from Sinopharm Chemical.

Synthesis of gPEA-SH. gPEA-SH was synthesized according to the previous report.[44] Typically, to a 50 mL two-neck flask equipped with a nitrogen inlet tube and a reflux condenser, PPO−DE, Jaffamine L100 and AET were added to the flask in proportion (shown in Table 1), and then ethanol was added. The total monomer concentration was kept at 0.5 g/mL. The mixture was refluxed for 12 h, and then poured into *n*-hexane. After removing the supernatant, gPEA-SH was collected and dried.

Synthesis of TMS-gPEAs. To the solution of toluene with trace of photoinitiator I-907, gPEA-SH and MPS (thiol/acrylate = 1:1.3) were added. The mixture was irradiated by 365 nm ultraviolet light for 12 h. Then the mixture was poured into *n*-hexane. After removing the supernatant, the graft polymer containing trimethoxysilyl moiety (TMS-gPEA) was collected and dried.

Formation of the Hybrid Nanoparticles ($SiO_{1.5}$-gPEAs). The hydrolysis and condensation of TMS-gPEAs was conducted in one pot by direct dispersion in water. The polymer was dispersed in aqueous solution immediately to form transparent solution, followed by gradual hydrolysis and condensation of the trimethoxysilyl groups for 3 days to form the core cross-linked hybrid $SiO_{1.5}$-gPEA NPs

Separation Experiment. To 4 mL of dye aqueous solution with concentration of 0.15 mg/mL in centrifuge tube, 40 mg $SiO_{1.5}$-gPEA11 NPs was added. After heating at 80 °C for 10 min, the turbid solution was centrifuged. Meanwhile, the UV−vis spectra of dye in initial aqueous solution with or without $SiO_{1.5}$-gPEA11 as well as in supernatant after centrifugation were recorded. The separation efficiency (Φ) of water-soluble dyes was defined as the following eq 1:

$$\phi = \frac{C_0 - C_s}{C_0} \times 100\% \quad (1)$$

Here C_0 is the dye's concentration in the initial solution and C_s is the dye's concentration in the supernatant. The concentration of dye in the supernatant and in the initial solution could be determined by the UV−vis spectra.

Characterization. ^{1}H nuclear magnetic resonance spectroscopy (^{1}H NMR) measurements were carried out on a Varian Mercury Plus spectrometer, operating at 400 MHz by using $CDCl_3$ as solvent and tetramethylsilane as an internal standard. Fourier transform infrared spectroscopy (FT-IR) spectra of products were recorded on a Perkin-Elmer Paragon1000 FT-IR spectrometer. Molecular weights (M_n) and molecular weight distributions (M_w/M_n) were determined by a Serious 200 gel permeation chromatography (GPC) with differential refractometer as the detector. *N,N*-Dimethylformamide (DMF) was used as the eluent at a flow rate of 1.0 mL/min and polystyrene as the calibration standard. Transmission electron microscopy (TEM) was carried out on JEOL JEM-2100 microscope, operating at 200 kV. A drop of 1 mg/mL $SiO_{1.5}$-gPEA NPs aqueous solution was placed onto a copper grid and the excess solution was removed by a filter paper.

Cloud Point (CP) Measurements. The optical transmittance of the polymer solutions were measured at 500 nm with a UV-2550 spectrophotometer (Shimadzu, Japan) equipped with circulating water bath. The temperature at 90% light transmittance of the polymer solution was defined as the CP. The copolymer aqueous solutions were prepared from 0.1 M citrate buffered aqueous solutions with 0.3 wt % copolymer concentration.

Dynamic Light Scattering (DLS). The measurements were performed in the 1 mg/mL copolymer solution with pH 7.0 using a Zetasizer Nano ZS90 instrument (Malvern Instruments) equipped with a 4 mW He−Ne laser (λ = 633 nm) at an angle of 90°, an avalanche photodiode detector with high quantum efficiency, and an ALV/LSE-5003 multiple τ digital correlator electronics system. Regularized Laplace inversion (CONTIN algorithm) was applied to analyze the obtained autocorrelation functions. The size of the nanoparticles was determined using the volume-weighted distribution of particle sizes.

Results and Discussion

Synthesis and Characterization of TMS-gPEAs. The strategy for synthesis of TMS-gPEAs is illustrated in Scheme 1. We synthesized three gPEA-SHs containing different amount of thiol groups, which were named as gPEA-SH11, gPEA-SH12, and gPEA-SH13, respectively. Their component and molecular weight (M_n) are summarized in Table 1. Accordingly, the synthesized TMS-gPEAs containing TMS moieties in side-chains were named as TMS-gPEA11, TMS-gPEA12, and TMS-gPEA13. The structure of TMS-gPEAs was confirmed by FT-IR and ^{1}H NMR. As shown in the FT-IR spectra (Figure 1), the bands at 3441, 1726, and 1109 cm^{-1} are attributed to stretching vibration of O−H, C═O, and C−O−C in TMS-gPEAs, respectively. Compared to gPEA-SH11, the appearance of peak at 1726 cm^{-1} (C═O) in the FT-IR spectra of TMS-gPEAs indicates the successful introduction of TMS moieties into the copolymers. From TMS-gPEA13 to TMS-gPEA11, the band at 1726 cm^{-1} increases obviously. The successful synthesis of TMS-gPEAs is further confirmed by ^{1}H NMR. As shown in Figure 2, the peak of TMS-gPEA11 assigned to Hd (δ = 0.6 ppm) appears after the "thiol−ene" reaction of gPEA-SH11 with MPS. From TMS-gPEA13 to TMS-gPEA11, the peak (δ = 0.6 ppm) becomes more obvious with the increasing amount of TMS moieties, which is in good agreement with the result from FT-IR.

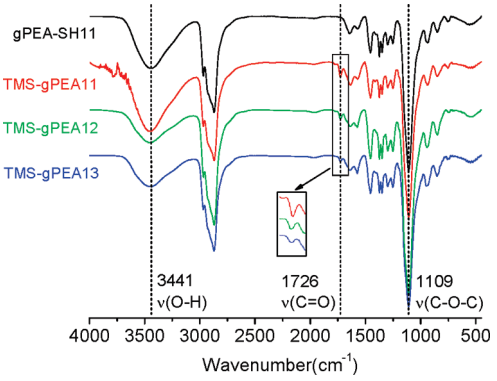

Figure 1. FT-IR spectra of gPEA-SH11 and TMS-gPEAs.

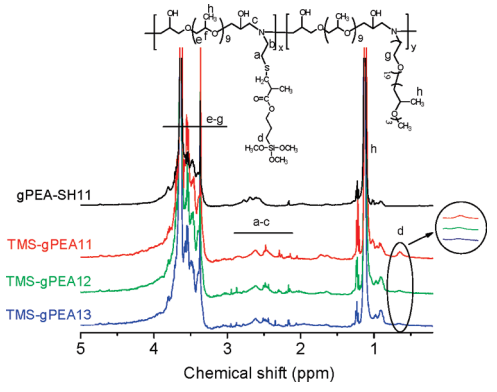

Figure 2. ^{1}H NMR spectra of gPEA-SH11 and TMS-gPEAs in $CDCl_3$.

Formation of the Hybrid $SiO_{1.5}$-gPEAs NPs. TMS-gPEAs are comprised of hydrophilic L100 as graft chain, and hydrophobic PPO backbone and TMS moieties in side chain. Just like other amphiphilic PEAs, TMS-gPEAs could be dispersed directly into water to form nanoparticles with hydrophobic PPO and TMS as core and hydrophilic L100 as shell. The hydrophobic core can be further cross-linked through hydrolysis and condensation of TMS moieties for 3 days. It should be noted that no other catalyst such as ammonia was added for hydrolysis of TMS moieties due to the existence of amine groups in TMS-gPEAs. The whole strategy for formation of hybrid core-cross-linked nanoparticles ($SiO_{1.5}$-gPEA NPs) is illustrated in Scheme 2. The morphology and size distribution of the obtained hybrid nanoparticles ($SiO_{1.5}$-gPEA NPs) were revealed by TEM and DLS. Figure 3 shows the representative TEM images of $SiO_{1.5}$-gPEAs in aqueous and tetrahydrofuran (THF) solution. In aqueous solution, the diameter of $SiO_{1.5}$-gPEA13, $SiO_{1.5}$-gPEA12, and $SiO_{1.5}$-gPEA11 nanoparticles are 22.4 ± 2.2 nm, 22.8 ± 3.5 nm and 24.2 ± 2.3 nm, respectively. According to DLS results (Figure 4), the *Z*-average diameters of $SiO_{1.5}$-gPEA13, $SiO_{1.5}$-gPEA12, and $SiO_{1.5}$-gPEA11 nanoparticles in aqueous solution are 17.6 ± 6.3, 21.7 ± 6.1, and 22.5 ± 5.8 nm with low polydispersity index (PDI) of 0.420, 0.311, and 0.301, respectively, which is comparable to TEM results. The obtained $SiO_{1.5}$-gPEA11 particles do not even disassemble in good organic solvent such as THF, indicating the tight cross-linked core and its good stability. Figure 3D presents TEM image of $SiO_{1.5}$-gPEA11 in THF. Compared to $SiO_{1.5}$-gPEA11 in aqueous solution, the diameter in THF is 41.7 ± 5.7 nm, about twice larger than those in water (Figure 3A). This was further confirmed by the DLS results (Figure 4). The larger size of $SiO_{1.5}$-gPEA11 NPs in THF might be due to swelling of the cross-linked core in good solvent.

Responsive Aggregation Behaviors of Hybrid $SiO_{1.5}$-gPEAs NPs. The aggregation behaviors of $SiO_{1.5}$-gPEA NPs under different conditions were investigated. The obtained hybrid nanoparticles are comprised of hydrophobic organosilica and PPO backbones as core and hydrophilic L100 chain as outer shell, which prevents them to aggregate further. With the increase of temperature, the L100 outer shell becomes less hydrophilic because hydrogen bond between L100 chain and water can be destroyed at high temperature. Therefore, the nanoparticles will aggregate, resulting in turbidity of solution. To test the possibility of response to temperature, we checked the size distribution of

Scheme 2. Proposed Mechanism of Phase Transition of $SiO_{1.5}$-gPEAs Aqueous Solution

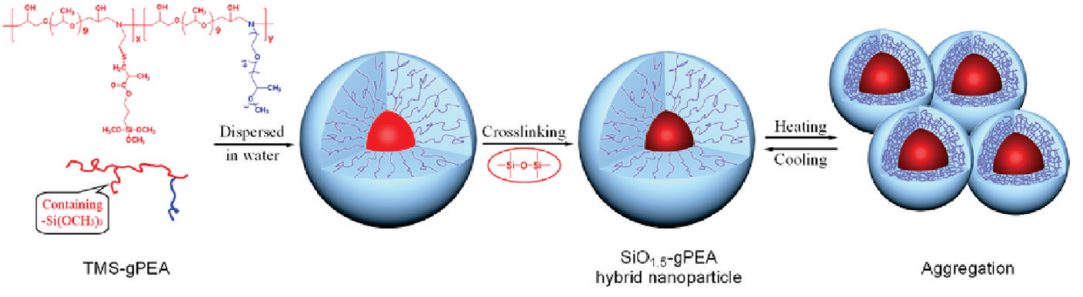

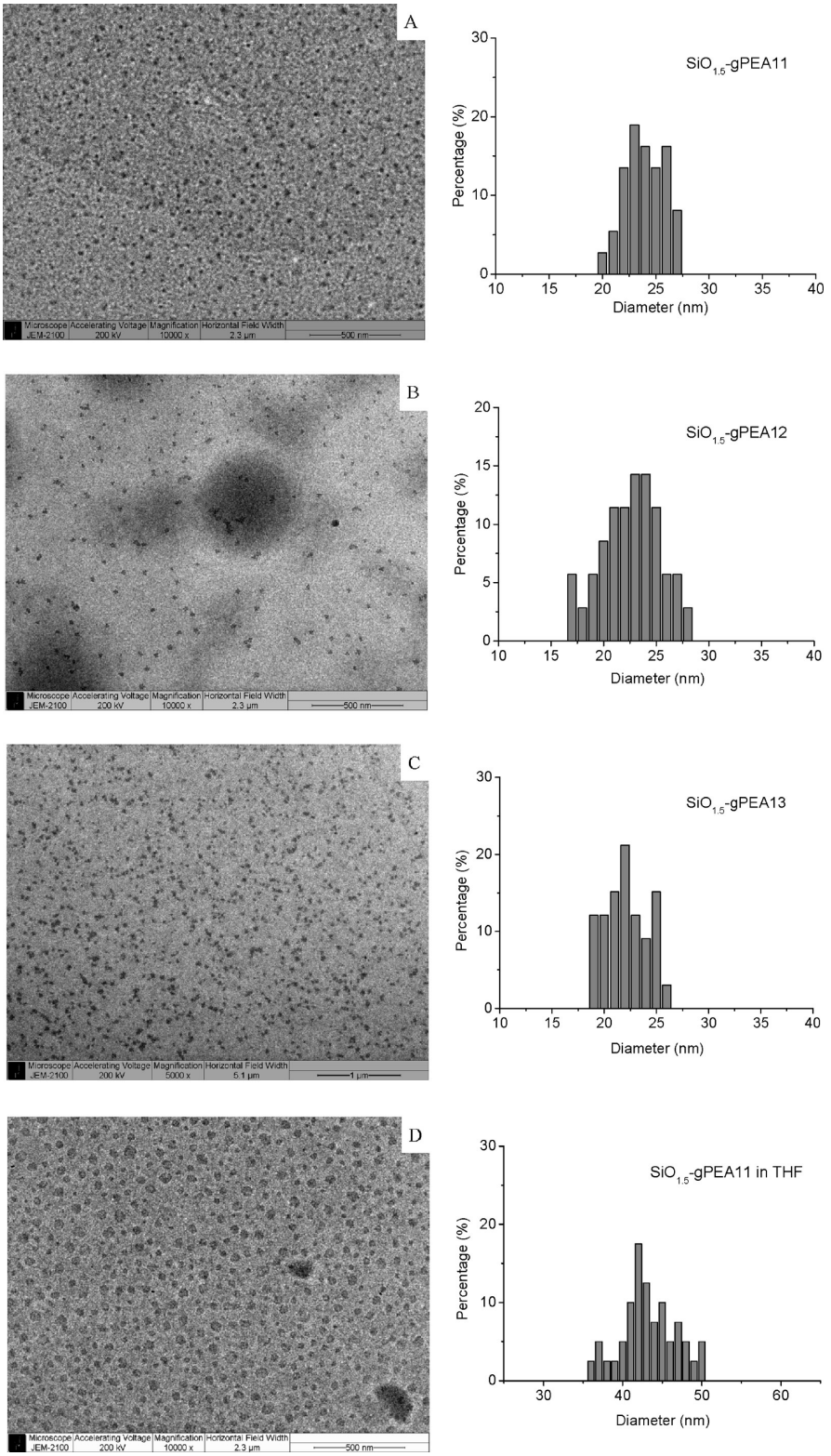

Figure 3. TEM images (left) and particle size distribution (right) of (A) $SiO_{1.5}$-gPEA11, (B) $SiO_{1.5}$-gPEA12, (C) $SiO_{1.5}$-gPEA13 in water, and (D) $SiO_{1.5}$-gPEA11 in THF at room temperature (c = 1 mg/mL). 35 particles were counted for size distribution.

$SiO_{1.5}$-gPEA11 nanoparticles in aqueous solution at the increasing temperature by DLS. As shown in Figure 5, $SiO_{1.5}$-gPEA11 aqueous solution was clear and transparent with size of ~20 nm in diameter at low temperature. When heated to 60 °C, the solution turned turbid and $SiO_{1.5}$-gPEA11 nanoparticles could aggregate into large particles with size of several micrometers in diameter. After cooling to room temperature, the solution turned to transparent again and $SiO_{1.5}$-gPEA11 returned to nanoparticles with diameter of ~20 nm (inset in Figure 5A). Figure 5C reveals the TEM image of the aggregation at high temperature. Because of their cross-linked organosilica core, $SiO_{1.5}$-gPEA11 could not fully integrate to form mesoglobules but irregular particles with obvious silica-contained cores.

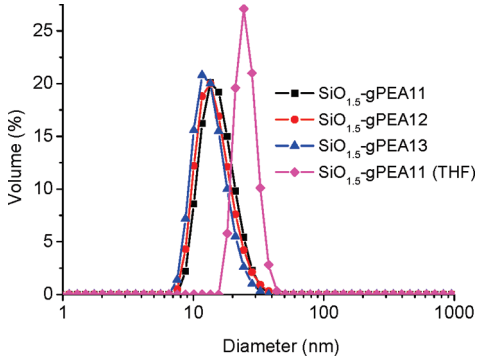

Figure 4. Volume-weighted size distribution of $SiO_{1.5}$-gPEAs aqueous and THF solution (c = 1 mg/mL) obtained by DLS at room temperature (pH = 7.0 in aqueous solution).

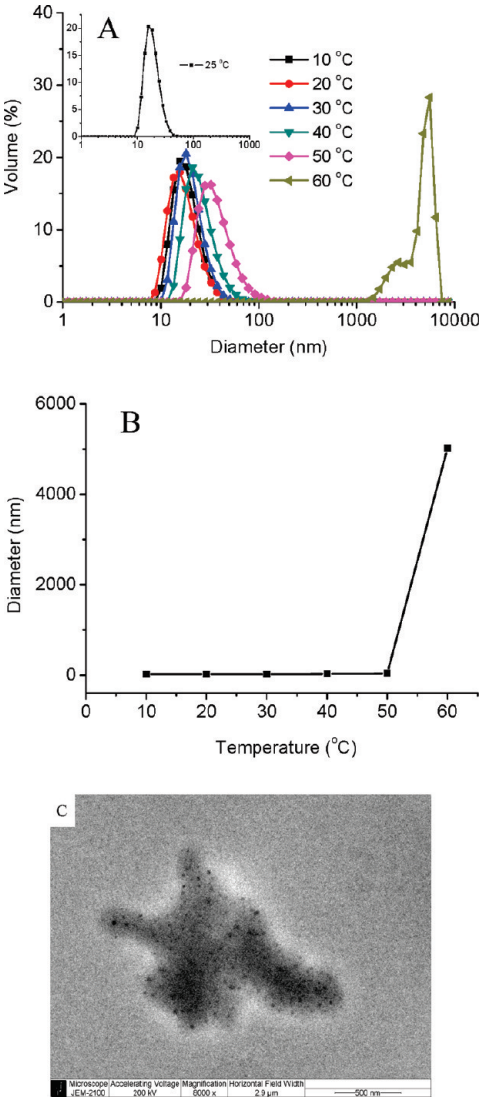

Figure 5. (A) Volume-weighted size distribution of $SiO_{1.5}$-gPEA11 aqueous solution obtained by DLS at different temperature, inset: size distribution of $SiO_{1.5}$-gPEA11 NPs aqueous solution cooling to 25 °C. (B) Temperature dependent size of $SiO_{1.5}$-gPEA11 NPs. (C) TEM image of $SiO_{1.5}$-gPEA11 at 70 °C. c = 1 mg/mL.

To investigate systematically the responsive aggregation behavior of $SiO_{1.5}$-gPEAs nanoparticles under different conditions, we recorded temperature dependent transmittance measurements by using UV−vis spectrometer. The

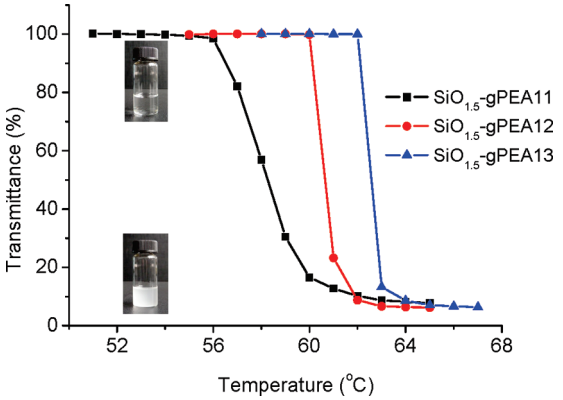

Figure 6. Optical transmittance at 500 nm vs temperature curves for 3 mg/mL $SiO_{1.5}$-gPEAs in aqueous solution at pH 7.0.

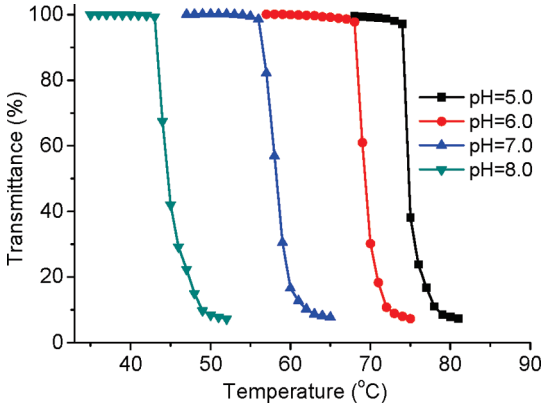

Figure 7. Optical transmittance at 500 nm vs temperature curves for 3 mg/mL $SiO_{1.5}$-gPEA11 in aqueous solution at different pH.

corresponding temperature dependence of transmittance for three aqueous solutions of $SiO_{1.5}$-gPEAs at pH 7.0 is shown in Figure 6, from which cloud point (CP) can be obtained. These solutions exhibit sharp transition from transparence to turbidity with increase of temperature, indicating the aggregation of $SiO_{1.5}$-gPEAs NPs. From $SiO_{1.5}$-gPEA13 to $SiO_{1.5}$-gPEA11. CP decreased with the increasing amount of hydrophobic TMS moieties.

Because of the tertiary amine moieties in the structure of $SiO_{1.5}$-gPEAs which can be protonated or deprotonated at different pH, $SiO_{1.5}$-gPEA NPs are expected to be responsive to pH.[34,45] Temperature dependence of transmittance for $SiO_{1.5}$-gPEA11 aqueous solutions at different pH was recorded by UV−vis spectra. As shown in Figure 7, the effect of pH on transition temperature of $SiO_{1.5}$-gPEA11 solution is very obvious, suggesting that CP can be controlled by pH: i.e., by increasing pH value, CP becomes lower accordingly. With the increasing pH value from 5.0 to 8.0, CP of $SiO_{1.5}$-gPEA11 decreases from 74.2 to 43.4 °C, indicating its sharp response to pH. CP of all $SiO_{1.5}$-gPEAs at different pH value is summarized in Table 2. For all $SiO_{1.5}$-gPEAs, the increasing pH value leads to the decrease of CP due to the deprotonation of amino groups at high pH. Size distribution of $SiO_{1.5}$-gPEA11 at different pH was also determined by DLS (Figure S1, Supporting Information), from which pH has no obvious effect on the size of $SiO_{1.5}$-gPEA11 nanoparticles in the range of measurement.

Because of the outer shell of L100 chain, the aggregation of $SiO_{1.5}$-gPEA nanoparticles is also expected to be sensitive to ionic strength, which is one of the dominating parameters in various aqueous system. Figure 8 shows transmittance

Table 2. CP of $SiO_{1.5}$-gPEAs Aqueous Solution at Different pH

	CP of $SiO_{1.5}$-gPEAs aqueous solution at different pH (°C)			
polymer	pH = 8.0	pH = 7.0	pH = 6.0	pH = 5.0
$SiO_{1.5}$-gPEA11	43.4	56.5	68.2	74.2
$SiO_{1.5}$-gPEA12	53.1	60.1	69.0	76.1
$SiO_{1.5}$-gPEA13	56.1	62.2	71.1	79.3

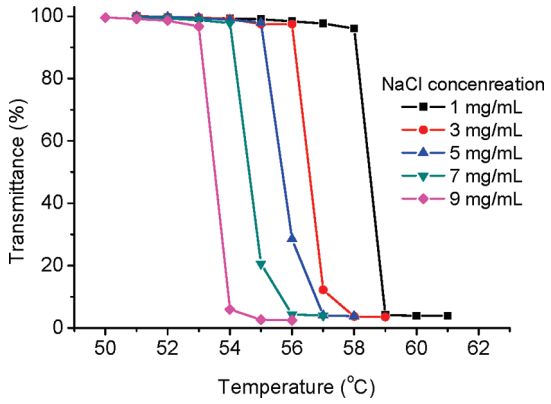

Figure 8. Optical transmittance at 500 nm vs temperature curves for 3 mg/mL $SiO_{1.5}$-gPEA11 in aqueous solution at different NaCl concentrations.

versus temperature curves of $SiO_{1.5}$-gPEA11 with different NaCl concentration. $SiO_{1.5}$-gPEA11 exhibits very sharp phase transition in wide range of NaCl concentration when heated. CP decreased with the increasing NaCl concentration because of partial dehydration of polymer chain. These results can be explained by salting-out effect.[46] With the increasing NaCl concentration from 0 mg/mL to 9 mg/mL, CP decreases from 58.1 to 53.0 °C. Lutz et al. reported that CP of copolymer containing PEO short chain decreased from 37.5 to 34.5 °C with the increasing NaCl concentration from 0 to 11 mg/mL.[47] Compared to Lutz's results, $SiO_{1.5}$-gPEAs NPs are responsive to ionic strength more significantly. We also checked the size distribution of $SiO_{1.5}$-gPEA11 at different NaCl concentration by DLS (Figure S2, Supporting Information), and found that ionic strength has no obvious effect on the size of $SiO_{1.5}$-gPEA11 nanoparticles in the range of measurement.

On the basis of the above studies, we proposed the possible transition process of $SiO_{1.5}$-gPEA nanoparticles in aqueous solution, which is illustrated in Scheme 2. At room temperature $SiO_{1.5}$-gPEAs were dispersed as nanoparticles in water with hydrophobic core of PPO backbones and robust organosilica cross-links and hydrophilic shell of L100. Raising temperature higher than their CP, the L100 graft chains become less hydrophilic, resulting in aggregation to form microparticles. The process is thermal-reversible, which means $SiO_{1.5}$-gPEAs can return to nanoparticles after cooling. Furthermore, if the hydrolysis and condensation of TMS-gPEAs were conducted at temperature higher than their CP, we could obtain much larger $SiO_{1.5}$-gPEAs particles (~700 nm in diameter). The detailed DLS and TEM date of the obtained microparticles were outlined in the Supporting Information (Figure S3 and S4).

Smart Separation and Transfer of Dyes. Because of the excellent performance of response to temperature, pH and ionic strength, $SiO_{1.5}$-gPEAs are expected to be potential in applications such as controlled drug delivery and separation.[10,48,49] Just like polymeric micelles formed by self-assembly of other amphiphilic poly(ether amine)s in water,[40,41] the

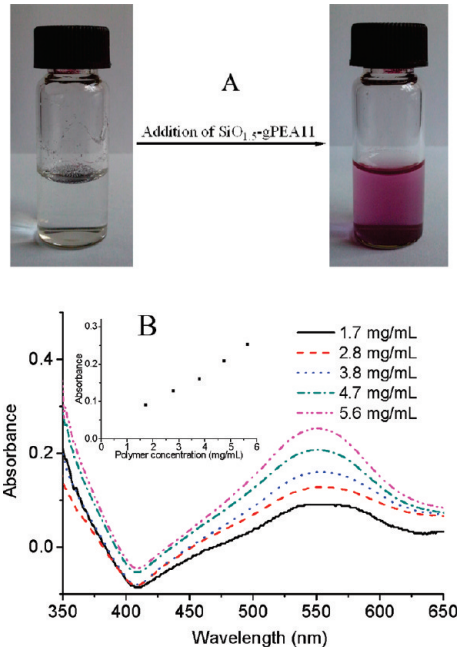

Figure 9. Encapsulation of hydrophobic guest molecules. (A) Photographs of Nile Red in water before (left) and after (right) the addition of $SiO_{1.5}$-gPEA11. (B) UV−vis spectra of Nile Red dispersed in water by various concentrations of $SiO_{1.5}$-gPEA11. Inset: plots of maximum absorbance of Nile Red vs $SiO_{1.5}$-gPEA11 concentration.

robust hybrid $SiO_{1.5}$-gPEAs core-cross-linked nanoparticles could encapsulate hydrophobic guest molecules in water. As Figure 9A shows, hydrophobic Nile Red which is insoluble in water, could be dispersed immediately in water in the presence of $SiO_{1.5}$-gPEA11 NPs, which can be reflected by change of the solution's color visible to eye. This could also be proved by UV−vis spectra (Figure 9B). Upon addition of $SiO_{1.5}$-gPEA11, the absorption band at ~550 nm increases with the increasing $SiO_{1.5}$-gPEA11 concentration. The dispersion behavior of Nile Red in water in presence of $SiO_{1.5}$-gPEA11 can be explained by the encapsulation properties of nanoparticles. Hydrophobic dye Nile Red can be encapsulated in hydrophobic core of $SiO_{1.5}$-gPEA11 in water, resulting in good dispersion of Nile Red in water.

On the other hand, hydrophilic dyes could also be incorporated into the amphiphilic nanoparticles. Maskos et al. reported on a kind of amphiphilic polymeric core−shell nanocontainers with ammonium groups contained hydrophilic core and nonpolar shell.[50,51] The hydrophilic dyes could be incorporated into the particle's core, resulting in the dissolution of hydrophilic dyes in organic solvents. So it is interesting to know whether or not hydrophilic dyes can be encapsulated in our hybrid nanopartilces. To verify this idea, we dissolved the water-soluble dye Rose Bengal (RB) in $SiO_{1.5}$-gPEA11 aqueous solution and covered it with an apolar solvent such as toluene, in which the dye is known to be insoluble. After heating at 80 °C for 10 min, the mixture was stirred, followed by centrifuging to yield the phase-separated mixture. The coloration of the toluene phase and decoloration of the aqueous phase were observed, indicating the transfer of RB from aqueous phase to the toluene phase (Figure 10A,B). After cooling to room temperature, the toluene phase could return to colorless, indicating the redissolution of RB in aqueous solution. Our previous study indicated that gold nanoparticles with amphiphilic responsive poly(ether amine)s as the protected shell possessed reversible phase transition property in water/toluene solution.[44] So we

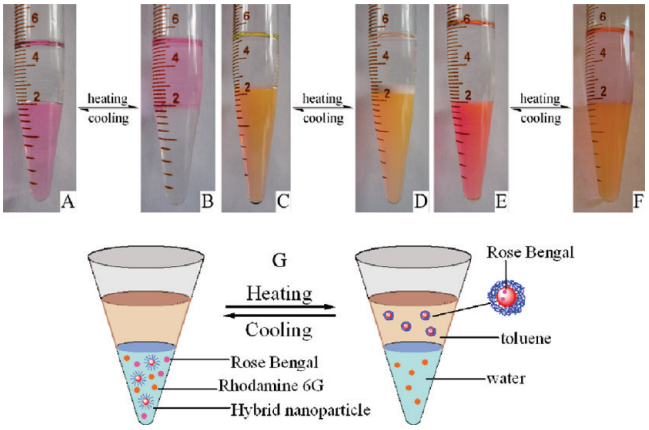

Figure 10. Photograph of the dye transfer between toluene and water phase at low temperature (left) and high temperature (right): (A and B) Rose Bengal; (C and D) Rhodamine 6G; (E and F) Rose Bengal and Rhodamine 6G mixture. (G) Proposed mechanism for the dye transfer.

proposed that the hydrophilic dye RB was sequestered in the $SiO_{1.5}$-gPEA11 nanoparticles and migrated with them, which can be controlled by temperature. The similar experiment was also carried out by using a cationic dye Rhodamine 6G (R6G). In contrast, R6G did not transfer to the toluene phase after heating and centrifugation (Figure 10C,D). This was an interesting phenomenon. R6G could not be encapsulated in the $SiO_{1.5}$-gPEA11 nanoparticles while RB exhibited strong ability to be encapsulated, indicating that $SiO_{1.5}$-gPEA11 nanoparticles possess the unique selective encapsulation of hydrophilic dye in water.

Motivated by the unique selective encapsulation of hydrophilic dye, we tried to use $SiO_{1.5}$-gPEA11 nanoparticles to separate RB/R6G in their mixture aqueous solution. To test this possibility, both RB and R6G were dissolved in the aqueous phase, it is obvious that only RB (purple dye) migrated to the toluene phase while R6G (orange dye) was left in the aqueous phase (Figure 10E,F) after heating. The proposed mechanism for separation is illustrated in Figure 10G.

To further understand the selective encapsulation of hydrophilic dye in water, we did the separation experiment directly in aqueous solution and checked the UV−vis spectra of hydrophilic dyes in pure water, as well as in $SiO_{1.5}$-gPEA11 aqueous solution before and after separation (Figure 11). As for RB, after heating and centrifugation most of the dye precipitated or adhered to the centrifuge tube wall, and the supernatant was almost colorless. Compared to the initial RB/$SiO_{1.5}$-gPEA11 solution, the absorbance of the supernatant decreased significantly, and the separation efficiency was 90%. It is notable that after adding $SiO_{1.5}$-gPEA11 the maximum absorption wavelength (λ_{max}) red-shifted from 546 to 561 nm, which is close to RB absorption in medium polar solution THF (λ_{max} = 562 nm). The significant red-shifted λ_{max} of RB in the presence of $SiO_{1.5}$-gPEA11 might be ascribed to the change of microenvironment of RB in water, indicating that RB were sequestered as guests into the hydrophobic core of $SiO_{1.5}$-gPEA11, and precipitated with them at temperature higher than CP. The polarity of the nanoparticles' core comprised of PPO chain is similar to THF. Although RB is hydrophilic, the polarity of RB might be comparable to THF and the core of $SiO_{1.5}$-gPEA11, and the negatively charged RB molecules could also be adsorbed by the positively charged core of $SiO_{1.5}$-gPEA11 due to the amine groups. As for R6G, the dye did not precipitate after heating and centrifugation. UV−vis spectra (Figure 11B) also show that after adding $SiO_{1.5}$-gPEA11 the

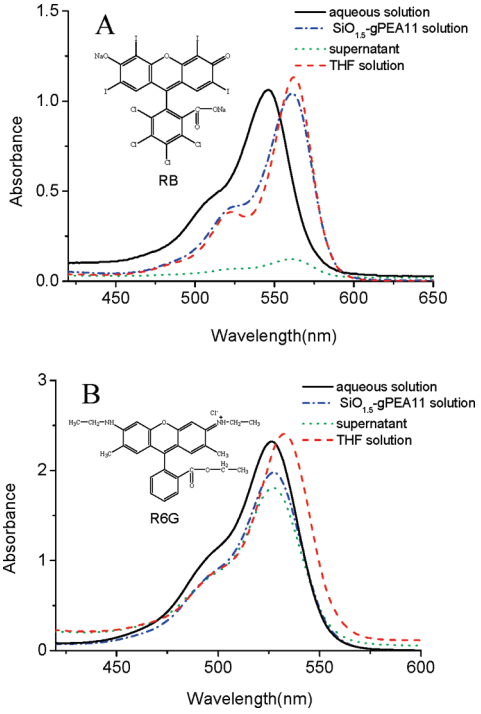

Figure 11. UV−vis spectra of (A) Rose Bengal and (B) Rhodamine 6G solution in separation experiment ($c_{SiO1.5\text{-}gPEA11}$ = 10 mg/mL, c_{dye} = 0.15 mg/mL). Initial dye in pure water (solid line); dye in $SiO_{1.5}$-gPEA11 solution (dash dot line); dye in supernatant after heating and centrifugation (dot line); dye in THF solution (dash line).

maximum absorption wavelength (λ_{max}) red-shifts slightly from 526 to 527 nm, while λ_{max} of R6G in THF is 533 nm. The relative red-shift value of RB (15 nm in the presence of $SiO_{1.5}$-gPEA11; 16 nm in THF) is much greater than that of R6G (1 nm in the presence of $SiO_{1.5}$-gPEA11; 7 nm in THF), indicating the almost no interaction between R6G and the core of $SiO_{1.5}$-gPEA11.

To find the factors to determine the unique selectivity, more separation experiments of four other hydrophilic dyes were tested and their UV−vis spectra were recorded in Figure S5 (Supporting Information). As for anionic dyes Amido Black 10B (10B) and Bordeaux R (BoR), most of 10B precipitated with separation efficiency of 85% while the separation efficiency of BoR is 52%. Similar to RB, an obvious red-shift of 10B was observed after adding $SiO_{1.5}$-gPEA11, which means 10B is also encapsulated into the core of the nanoparticles. However, this phenomenon is not observed for BoR, which might be due to sole adsorption. As for amine group-contained dyes Methyl Orange (MO) and Calcein (Cl), the separation efficiency is low (35% and 21%). However, the slight blue-shift of MO absorption from 464 to 457 nm means that a part of dye molecules could also be encapsulated into the core of nanoparticles. Compared to that in pure water, there is no shift of Cl absorption in $SiO_{1.5}$-gPEA11 aqueous solution, indicating no encapsulation of Cl in the core. At the same time, the amine groups in Cl reduce its adsorption in the surface of $SiO_{1.5}$-gPEA11 nanoparticles, resulting in the low separation efficiency.

The reasons why $SiO_{1.5}$-gPEA NPs exhibited the unique selective encapsulation of hydrophilic dyes were not completely clear. Taking the structure of dyes and their separation efficiency into consideration, however, we propose that the interaction between dyes and $SiO_{1.5}$-gPEAs nanoparticles include two factors: (1) Charge-based specificity.[50−52] The ionic interactions between the positively charged

ammonium groups of the nanoparticles and the negatively charged groups of the dye are the important factor. Negatively charged dyes such as RB and 10B showed separation efficiency higher than 85%. In contrast, positively charged or amine group-contained dyes showed low separation efficiency (lower than 35%). (2) Structure of the dyes such as the polarity and their interaction with $SiO_{1.5}$-gPEAs' core. We observed that for negatively charged BoR the separation efficiency is only 52%. This might be due to no encapsulation of dye molecules into the nanoparticles' core. So in addition to ionic interaction, the structure of the dyes such as the polarity is also of importance for loading. In summary, negatively charged dyes such as RB and 10B, which could be encapsulated into the nanoparticles' core showed remarkable separation efficiency higher than 85%, while positively charged dyes such as R6G, which could not be encapsulated into the nanoparticles' core showed almost no separation efficiency.

Conclusions

We prepared a series of amphiphilic organosilica hybrid nanoparticles that contain robust silsesquioxane network and hydrophobic PPO as the core and hydrophilic L100 as the shell. The obtained hybrid nanoparticles exhibited response to ionic strength, especially sharp response to temperature and pH. The hybrid nanoparticles exhibited unique encapsulation selectivity for different hydrophilic dyes, and can separate RB and R6G in the aqueous solution by controlling temperature. This property provides a unique handle for smart separation. Further work will be conducted on the factors to determine the unique selectivity of encapsulation.

Acknowledgment. We thank the National Nature Science Foundation of China (No: 50803036) and Science & Technology Commission of Shanghai Municipal Government (No: 08520704700) for their financial support.

Supporting Information Available: Plots of *Z*-average diameter of $SiO_{1.5}$-gPEA11 nanoparticles under different pH and ionic strength by DLS, a TEM image, volume-weighted size distribution of $SiO_{1.5}$-gPEA11 microparticles for hydrolysis and condensation at high temperature, and UV−vis spectra of four other hydrophilic dyes in separation experiment. This material is available free of charge via the Internet at http://pubs.acs.org.

References and Notes

(1) Boury, B.; Corriu, R. J. P.; Le Strat, V.; Delord, P.; Nobili, M. *Angew. Chem., Int. Ed.* **1999**, *38*, 3172–3175.
(2) Du, J. Z.; Chen, Y. M. *Angew. Chem., Int. Ed.* **2004**, *43*, 5084–5087.
(3) Descalzo, A. B.; Martinez-Manez, R.; Sancenon, F.; Hoffmann, K.; Rurack, K. *Angew. Chem., Int. Ed.* **2006**, *45*, 5924–5948.
(4) Caruso, F. *Adv. Mater.* **2001**, *13*, 11–22.
(5) Sanchez, C.; Julian, B.; Belleville, P.; Popall, M. *J. Mater. Chem.* **2005**, *15*, 3559–3592.
(6) Sanchez, C.; Soler-Illia, G. J. de A. A.; Ribot, F.; Lalot, T.; Mayer, C. R.; Cabuil, V. *Chem. Mater.* **2001**, *13*, 3061–3083.
(7) Lin, W. C.; Fan, W.; Marcellan, A.; Hourdet, D.; Creton, C. *Macromolecules* **2010**, *43*, 2554–2563.
(8) Hoffmann, F.; Cornelius, M.; Morell, J.; Froba, M. *Angew. Chem., Int. Ed.* **2006**, *45*, 3216–3251.
(9) Du, J. Z.; Chen, Y. M. *Macromolecules* **2004**, *37*, 5710–5716.
(10) Huo, Q. S.; Liu, J.; Wang, L. Q.; Jiang, Y. B.; Lambert, T. N.; Fang, E. *J. Am. Chem. Soc.* **2006**, *128*, 6447–6453.
(11) Mullner, M.; Schallon, A.; Walther, A.; Freitag, R.; Mullner, A. H. E. *Biomacromolecules* **2010**, *11*, 390–396.
(12) Lee, J.; Park, J. C.; Bang, J. U.; Song, H. *Chem. Mater.* **2008**, *20*, 5839–5844.
(13) Joo, S. H.; Park, J. Y.; Tsung, C. K.; Yamada, Y.; Yang, P.; Somorjai, G. A. *Nat. Mater.* **2009**, *8*, 126–131.
(14) Tan, H.; Liu, N. S.; He, B.; Wong, S. Y.; Chen, Z. K.; Li, X.; Wang, J. *Chem. Commun.* **2009**, 6240–6242.
(15) Yuan, J. Y.; Schacher, F.; Drechsler, M.; Hanisch, A.; Lu, Y.; Ballauff, M.; Mullner, A. H. E. *Chem. Mater.* **2010**, *22*, 2626–2634.
(16) Zhang, K.; Wu, W.; Guo, K.; Chen, J. F.; Zhang, P. Y. *Langmuir* **2010**, *26*, 7971–7980.
(17) Jovanovic, A. V.; Flint, J. A.; Varshney, M.; Morey, T. E.; Dennis, D. M.; Duran, R. S. *Biomacromolecules* **2006**, *7*, 945–949.
(18) Ow, H.; Larson, D. R.; Srivastava, M.; Baird, B. A.; Webb, W. W.; Wiesner, U. *Nano Lett.* **2005**, *5*, 113–117.
(19) Mohanraj, V. J.; Barnes, T. J.; Prestidge, C. A. *Int. J. Pharm.* **2010**, *392*, 285–293.
(20) Kasgoz, H.; Orbay, M. *Polymer* **2003**, *44*, 1785–1793.
(21) Jeong, B.; Gutowska, A. *Trends Biotechnol.* **2002**, *20*, 305–311.
(22) Haag, R. *Angew. Chem., Int. Ed.* **2004**, *43*, 278–282.
(23) Lutz, J. F. *Polym. Int.* **2006**, *55*, 979–993.
(24) Griset, A. P.; Walpole, J.; Liu, R.; Gaffey, A.; Colson, Y. L.; Grinstaff, M. W. *J. Am. Chem. Soc.* **2009**, *131*, 2469–2471.
(25) Chen, W.; Meng, F. H.; Li, F.; Ji, S. J.; Zhong, Z. Y. *Biomacromolecules* **2009**, *10*, 1727–1735.
(26) Aryal, S.; Hu, C. M. J.; Zhang, L. F. *ACS Nano* **2010**, *4*, 251–258.
(27) Hu, J. M.; Liu, S. Y. *Macromolecules* **2010**, *43*, 8315–8330.
(28) Allen, C.; Maysinger, D.; Eisenberg, A. *Colloids Surf. B* **1999**, *16*, 3–27.
(29) O'Reilly, R. K.; Hawker, C. J.; Wooley, K. L. *Chem. Soc. Rev.* **2006**, *35*, 1068–1083.
(30) Mori, H.; Muller, A. H. E.; Klee, J. E. *J. Am. Chem. Soc.* **2003**, *125*, 3712–3713.
(31) Du, J. Z.; Chen, Y. M.; Zhang, Y. H.; Han, C. C.; Fischer, K.; Schmidt, M. *J. Am. Chem. Soc.* **2003**, *125*, 14710–14711.
(32) McHale, R.; Chasdian, N.; Hondow, N. S.; Richardson, P. M.; Voice, A. M.; Brydson, R.; Wang, X. S. *Macromolecules* **2010**, *43*, 6343–6347.
(33) Mori, H.; Lanzendorfer, M. G.; Muller, A. H. E. *Macromolecules* **2004**, *37*, 5228–5238.
(34) Zhang, Y. F.; Luo, S. Z.; Liu, S. Y. *Macromolecules* **2005**, *38*, 9813–9820.
(35) Chung, P. W.; Kumar, R.; Pruski, M.; Lin, V. S. Y. *Adv. Funct. Mater.* **2008**, *18*, 1390–1398.
(36) Wei, H.; Cheng, Cheng; Chang, C.; Chen, W. Q.; Cheng, S. X.; Zhang, X. Z.; Zhuo, R. X. *Langmuir* **2008**, *24*, 4564–4570.
(37) Du, J. Z.; Armes, S. P. *J. Am. Chem. Soc.* **2005**, *127*, 12800–12801.
(38) Schumacher, M.; Ruppel, M.; Yuan, J.; Schmalz, H.; Colombani, O.; Drechsler, M.; Muller, A. H. E. *Langmuir* **2009**, *25*, 3407–3417.
(39) Ren, Y. R.; Jiang, X. S.; Yin, J. *J. Polym. Sci., Part A: Polym. Chem.* **2009**, *47*, 1292–1297.
(40) Ren, Y. R.; Jiang, X. S.; Liu, R.; Yin, J. *J. Polym. Sci., Part A: Polym. Chem.* **2009**, *47*, 6353–6361.
(41) Ren, Y. R.; Jiang, X. S.; Yin, G. L.; Yin, J. *J. Polym. Sci., Part A: Polym. Chem.* **2010**, *48*, 327–335.
(42) Jiang, X. S.; Wang, R.; Ren, Y. R.; Yin, J. *Langmuir* **2009**, *25*, 9629–9632.
(43) Goldmann, A. S.; Walther, A.; Nebhani, L.; Joso, R.; Ernst, D.; Loos, K.; Barner-Kowollik, C.; Barner, L.; Muller, A. H. E. *Macromolecules* **2009**, *42*, 3707–3714.
(44) Wen, Y. N.; Jiang, X. S.; Yin, G. L.; Yin, J. *Chem. Commun.* **2009**, 6595–6597.
(45) Liu, S. Y.; Armes, S. P. *Angew. Chem., Int. Ed.* **2002**, *41*, 1413–1416.
(46) Durme, K. V.; Rahier, H.; Mele, B. V. *Macromolecules* **2005**, *38*, 10155–10163.
(47) Lutz, J. F.; Akdemir, O.; Hoth, A. *J. Am. Chem. Soc.* **2006**, *128*, 13046–13047.
(48) Ganta, S.; Devalapally, H.; Shahiwala, A.; Amiji, M. *J. Controlled Release* **2008**, *126*, 187–204.
(49) Kataoka, K.; Harada, A.; Nagasaki, Y. *Adv. Drug Delivery Rev.* **2001**, *47*, 113–131.
(50) Jungmann, N.; Schmidt, M.; Ebenhoch, J.; Weis, J.; Maskos, M. *Angew. Chem., Int. Ed.* **2003**, *42*, 1714–1717.
(51) Gross, M.; Maskos, M. *Polymer* **2005**, *46*, 3329–3336.
(52) Tang, L. M.; Fang, Y.; Tang, X. L. *J. Polym. Sci., Part A: Polym. Chem.* **2005**, *43*, 2921–2930.